Available online at www.sciencedirect.com
SCIENCE DIRECT®
Catalysis Today 110 (2005) 92–97
CATALYSIS TODAY
www.elsevier.com/locate/cattod

Heterogeneous reactor model for steam reforming of methane in a microchannel reactor with microstructured catalysts

Chunshe Cao *, Yong Wang *, Robert T. Rozmiarek [1]

Institute of Interfacial Catalysis, Pacific Northwest National Laboratory, 902 Battelle Blvd., Richland, WA 99352, USA

Abstract

Microstructured catalysts used for methane steam reforming in microchannel reactors are mathematically described and experimentally demonstrated under realistic process conditions. A heterogeneous model has been developed with a graphical interface to represent the three dimensions of the microchannel reactor. Porous metal substrates (FeCrAlY) were used to form engineered catalysts with active precious metal (Rh) for methane steam reforming. Two types of structures were evaluated in the microchannel reactors and simulated with the developed heterogeneous reactor model. Local temperature and methane concentration profiles within the structures are illustrated to show the correlation of the catalyst structure and its performance. Such a modeling technique provides a convenient and flexible method to evaluate variables in designing more efficient catalysts for the highly endothermic steam reforming reactions, as the desired mass and heat transfer characteristics are achieved.

Keywords: Microstructured catalysts; Steam reforming; Heterogeneous model; Microchannel reactors

1. Introduction

Catalytic steam reforming of methane (SMR) produces synthesis gas (H_2 and CO) that is used for many important processes including methanol/dimethyl ether(DME) synthesis, ammonia production, and oxosynthesis of olefins to aldehydes [1]. Particularly, methane steam reforming provides feedstocks to the Fischer–Tropsch reactor for gas to liquid (GTL) conversion in stranded natural gas utilization [2]. Further, separation from syngas gives pure CO and H_2, which is widely used in varieties of organic chemical synthesis and petroleum processing such as carbonylation, hydrodesulphurization, hyrdrocracking, etc. [3]. Hydrogen is also the main energy carrier for fuel cells with no carbon emissions [4].

Commercial SMR processes use tubular reactors packed with supported nickel catalysts, as the supported precious metal catalysts are costly even though they have excellent steam reforming activity. In the conventional SMR reactors, strong endothermic reactions occur at high temperatures for high conversion with fast kinetics. As the SMR reaction becomes diffusion controlled in such regimes, engineering and optimization of catalyst structures play an important role in obtaining high activity and stability.

Conventional structured catalyst supports such as foams and monoliths used for gas-phase reactions, e.g., catalytic converters and volatile organic compound destruction, are generally ceramic-based. Although the ceramic support provides the advantages of low-pressure drop and high catalyst utilization efficiency, the poor heat transfer is still a problem resulting from low thermal conductivity. In recent years, microchannel reactors have been developed for process intensification and used in exothermic and endothermic reactions for their unprecedented temperature control and improved mass transfer [5–9]. The use of microchannel in SMR potentially minimizes the temperature gradient and allows the reaction occurring at a higher average temperature so that the process efficiency is enhanced. A metallic structured support, with its inherent high thermal conductivity, can be used as a substrate of catalysts and integrated for microchannel reactor applications. Thin layers of catalyst coating (typically <40 μm) on the metal substrate give much shorter transport distances than that of conventional catalysts [10]. In addition to better heat transfer, the sponge-like mechanical properties allow flexibility in sealing of catalysts in a reaction channel.

---

* Corresponding authors.
E-mail addresses: chunshecao@yahoo.com (C. Cao), yongwang@pnl.gov (Y. Wang).

[1] Present address: Virent Energy Systems Inc., 3571 Anderson Street, Madison, WI 53704, USA.

0920-5861/$ – see front matter © 2005 Elsevier B.V. All rights reserved.
doi:10.1016/j.cattod.2005.09.004

The closely matched thermal expansion between the structured metal supports and the housing reaction channels reduces the probability of structure cracking, which consequently minimizes gas channeling around the structured supports at higher reaction temperatures. The synergistically reduced resistance of mass/heat transfer in microchannel reactors and microstructured catalysts enhances the rate of the control step to match the fast reaction kinetics. This allows deployment of more active catalysts such as the use of precious metals. This paper describes a heterogeneous reactor model for steam reforming of methane with such microstructured catalysts in a microchannel reactor.

In developing microchannel reactors for the methane steam reforming, understanding the temperature profile within the reactor is important for designing and optimizing the catalysts structure to achieve the maximum performance. However, temperature measurement within the catalyst structures in such a small dimension becomes difficult, either due to insufficient room for a thermocouple or potential interference with local hydrodynamics. As the performance criteria such as conversion and selectivity are directly associated with the local temperature profiles, an accurate model is necessary.

As a mature technology, SMR kinetics and reactions in a conventional fixed bed have been well described [11,12]. Pseudo-homogeneous two-dimensional models have been used to simulate operation of the catalytic steam reformers [13,14]. Heterogeneous two-dimensional model accounting for the transport limitations at axial and radial reactor positions have been successfully used in simulating industrial steam reformers [15–17]. Numerous studies have focused on the kinetics of methane steam reforming [18–24], especially on Ni catalysts. Turnover rates for catalytically important noble metals (Rh, Pt, Ir, Ru) were reported recently [25], and the activity data for Rh/MgO/Al_2O_3 were shown in recent publications [26,27]. Nevertheless, modeling of methane steam reforming in a microchannel reactor is not currently available in the open literature. The purpose of the model discussed here is to illustrate the methane conversion and temperature distribution within the microstructure. A sensitivity study of the simulation can be used to tailor the catalyst structure to further reduce the mass/heat transfer limitation in the process and take advantage of the fast kinetics of the SMR reaction.

2. Experimental

2.1. Catalyst engineering

Two types of engineered catalysts (abbreviated as catalyst DF and catalyst C) were prepared based on FeCrAlY felts with different configurations in the microchannel reactor. The catalyst DF substrate consists of two single felts with identical dimensions (0.25 mm × 9 mm × 51 mm). Catalyst C is in a corrugated shape known as “ruffle.” The FeCrAlY felts used to make ruffles are also 0.25-mm thick. Ruffles have a fixed wavelength of 3 mm and fixed amplitude of 1.27 mm. The ruffles are 8.9 mm wide and 51 mm long. The schematics of both catalysts are shown in Fig. 1.

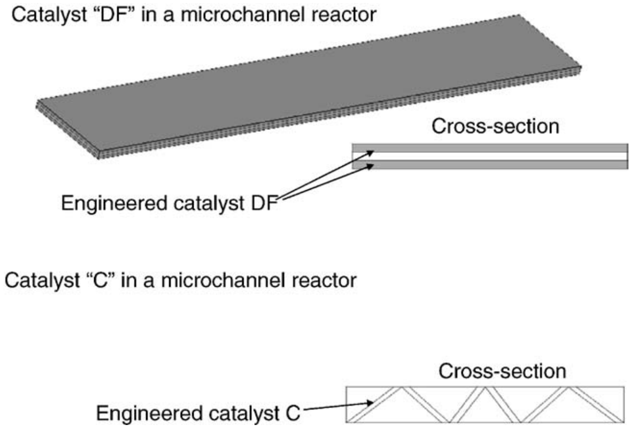

Fig. 1. Mirostructured catalysts in microchannel reactors.

A wash-coating procedure was used to apply a 10 wt% Rh/MgO/Al_2O_3 formulated catalyst onto both substrates. The catalyst preparation method is detailed elsewhere [10,26]; however, it is worth noting here that the catalyst particles in the washcoat were 1–3 μm, and about 14 mg of catalyst were wash-coated onto each square centimeter of the FeCrAlY felt surface.

2.2. Catalyst activity evaluation for steam reforming of methane

Catalyst activities were evaluated in microchannel reactors in a tube furnace. Catalyst DF felts were placed in a single channel reactor (0.75 mm × 9 mm × 51 mm) forming a gap of about 0.25 mm. It is important to ensure close contact between the felts and the walls for better heat transfer. Catalyst C was snug-fitted into a single channel reactor (1.27 mm × 8.9 mm × 51 mm) as a single ruffle, which confines the catalyst chamber volume. The catalyst chamber volume is defined as the single channel volume (0.75 mm × 9 mm × 51 mm for catalyst DF and 1.27 mm × 8.9 mm × 51 mm for catalyst C). Reactant gases flow in the direction perpendicular to the waves.

A mixture of methane and water (varying steam to carbon molar ratios) was introduced at gas hourly velocity (GHSV) varying from 144,000 to 3,600,000 h^{-1}. Gaseous methane feed was controlled by Brooks 5850E mass flow controllers. Water was introduced using an Acuflow Series III high performance liquid chromatograph pump. During the reaction, temperatures in the catalyst bed, bed inlet, and bed outlet were measured with type K thermocouples. The pressure drop across the bed was also recorded with pressure transducers (Noshok, 0–5v). Product gases were analyzed online by an Agilent Quad Micro gas chromatograph, which utilizes 5 A PLOT (MS-5A), PoraPLOTQ, PoraPLOTU, and OV-1 columns equipped with thermal conductivity detectors.

3. Reactor model

A three-dimensional heterogeneous model was used to describe the material and energy balance in the microchannel reactor system with structured catalysts. The model assumes that the variations of washcoat effective diffusivity, effective thermal conductivity, velocity, heat capacity, etc., are small, and the axial thermal conduction and diffusion are negligible compared to the convection. Constant velocity assumption was used for model simplicity. However, for a mole increase reaction-like SMR, 8% velocity increase can be a consequence of this simplification when temperature remains constant. As a matter of fact, for an endothermic reaction, the temperature drop in the bed greatly mitigates such a mole increase, and this 8% of velocity increase would be the worst case of scenario. Since the temperature profile is difficult to measure experimentally, the modeling effort intends to determine such endothermic effects. The empirical kinetic rate constant and apparent activation energy were used to express the first-order reaction with respect to methane. The following fundamental equations represent the conservation laws of mass and energy in the rectangular coordinates (x–y–z) with dependent variables: temperature T and methane concentration c.

In the gas phase:

$$u\frac{\partial c}{\partial z} = D_{\mathrm{mix}}\left(\frac{\partial^2 c}{\partial x^2} + \frac{\partial^2 c}{\partial y^2}\right) \tag{1}$$

$$u\rho C_{\mathrm{p}}\frac{\partial T}{\partial z} = k_{\mathrm{mix}}\left(\frac{\partial^2 T}{\partial x^2} + \frac{\partial^2 T}{\partial y^2}\right) \tag{2}$$

In the solid washcoat phase:

$$D_{\mathrm{eff}}\left(\frac{\partial^2 c}{\partial x^2} + \frac{\partial^2 c}{\partial y^2}\right) = k(c, T)c \tag{3}$$

$$k_{\mathrm{eff}}\left(\frac{\partial^2 T}{\partial x^2} + \frac{\partial^2 T}{\partial y^2}\right) = k(c, T)\, c(-\Delta H_{\mathrm{r}}) \tag{4}$$

where u is the linear velocity, D_{mix} the diffusivity of the gas mixture, D_{eff} the effective diffusivity in the catalyst washcoat phase, k_{mix} the thermal conductivity of the gas mixture, k_{eff} the effective thermal conductivity of the solid catalyst, and $(-\Delta H_{\mathrm{r}})$ the heat of reaction. Based on scaling analysis, the second derivates to z (axial diffusion and conduction) are three orders of magnitudes less than that to x and y directions. Therefore, axial diffusion and conduction were neglected in these mass and energy balance equations. This assumption is to parabolize the equations and makes them simpler to solve. The kinetics of methane steam reforming over the 10 wt% $Rh/MgO/Al_2O_3$ catalyst was measured by a microfixed bed reactor in which catalyst powder (80–100 mesh) was diluted with SiC particles for isothermal conditions (SiC/Cat = 3). The reaction rate was empirically correlated with the first-order kinetics to CH_4 with the frequency of $2.21 \times 10^{10}\ \mathrm{h}^{-1}$ (k_0) and the activation energy of 93 kJ/mol (E_{a}), so that the reaction rate constant k was expressed as the Arrhenius equation:

$$k(c, T) = k_0\, \mathrm{e}^{-E_{\mathrm{a}}/RT} \tag{5}$$

Diffusivities were calculated using molecular kinetics theory and Blanc's mixing law [28]. Knudsen diffusion occurring in the washcoat layers with pore size ranging from 20 to 200 Å are correlated with structure parameters such as porosity, density, tortuosity factor, and surface area. A typical value of the effective diffusion coefficient for the washcoat catalyst phase was $3.9 \times 10^{-3}\ \mathrm{cm^2/s}$ with 100 Å pore diameter and $1.65\ \mathrm{g/cm^3}$ bulk density. Such derived diffusion coefficients are tabulated in Table 1. Empirical values for effective thermal conductivities were used. Typical heat transfer parameters are listed in Table 2.

Table 1
Diffusion coefficients: $T = 850\ ^\circ\mathrm{C}$, $P = 20$ atm, gas composition: 6% CH_4, 24% H_2O, 5% CO_2, 12% CO, 53% H_2

Gas phase diffusivity (mixture); D ($\mathrm{cm^2/s}$)		0.1807		
Washcoat: effective diffusivity				
Pore size (Å)	20	100	150	200
D_{eff} ($\mathrm{cm^2/s}$)	0.000907	0.00387	0.00535	0.00654

The finite element solution algorithm was completed using FEMLAB (Comsol, Inc., version 3.0a). Multiphysics modules of convection–diffusion and conduction–convection were applied to the two-phase domains. For the simple geometry as a straight channel in the microchannel reactor, the three-dimensional (x, y, z) problem can be described by a two-dimensional (x, y) model using the time in the FEMLAB computing domain as the third dimension: z-axis This approach can be used because there is no second derivative in the z-axis. Therefore, with a two-dimensional reactor cross section in the Graphical User Interface of FEMLAB, coefficient and time-dependent partial differential equations are selected to represent such a heterogeneous catalytic structure. The transient solutions at different time steps represent the solutions at dimensionless spatial z-axis positions. In the FEMLAB GUI, the boundary conditions at the interface between the gas and solid phases are embedded in the multiphysics modules. At physical boundaries, the Neumann boundaries with zero conservative flux convection and source were used:

$$\vec{n} \cdot D\,\nabla c = 0 \tag{6}$$

Meshing parameters are listed as follows: predefined mesh sizes, normal; element growth rate, 1.3; mesh curvature factor, 0.3; mesh curvature cutoff, 0.001.

Table 2
Heat transfer parameters ($T = 850\ ^\circ\mathrm{C}$, $P = 20$ atm)

Reactor domain	Average gas density ρ at operating conditions ($\mathrm{kg/m^3}$)	Heat capacity of gas mixture, C_{p} (J/(mol K))	Thermal conductivity (W/(m-K))
Gas phase (6% CH_4, 24% H_2O, 5% CO_2, 12% CO, 53% H_2)	3.147	46.26	0.2
Solid phase			Effective thermal conductivity, k_{eff} (W/(m-K)) 16 [29]

4. Results and discussion

Methane steam reforming at 850 °C was used as a model reaction to evaluate the activities of the engineered catalysts. Table 3 shows methane steam reforming conversion on two types of engineered catalysts based on the FeCrAlY substrates. A steam to carbon ratio of 2 was maintained in the feed, and the reactor wall temperature was maintained at 850 °C. The contact time hereby is defined as the catalyst volume divided by the volumetric inlet gas flowrate at standard temperature and pressure, while the catalyst volume refers to the portion of the engineered catalyst that confines the single channel. The GHSV is thus the inverse of the "contact time." As shown in Table 3, as expected, methane conversion decreases with the increases of GHSV and pressure for the molar increasing endothermic equilibrium steam reforming reactions. Generally, catalyst DF is more active than catalyst C over the entire pressure range studied. Even at a shorter contact time of 3.8 ms, catalyst DF yields higher conversion than catalyst C at a longer contact time of 7.5 ms. The advanced performance of catalyst DF is attributed to many transport and reaction engineering factors. Apart from the lower catalyst loading on substrate C (geometric volume of the felt substrate: 0.15 cm^3 for catalyst C compared to 0.22 cm^3 for catalyst DF), most importantly, heat and mass transport played significant roles in coupling with the reaction kinetics. Numerical modeling of these two types of engineered catalysts can provide insights on explaining the differences in activity.

Table 3
Performance of the engineered catalysts [10] $T = 850$ °C, steam/C = 2

Catalyst	*P* (atm)	Contact time (ms)	Methane conversion (%)
DF	4	13.8	93
	4	3.8	74
	9	13.8	86
	10	3.8	72
	14	13.8	78
	17	3.8	64
	20	13.8	72
C	4	15	87
	4	7.5	64
	9	15	80
	9	7.5	60
	14	15	73
	14	7.5	57
	20	15	69
	20	7.5	54

Simulation revealed the local temperature and methane conversion profiles in the microchannel reactor with structured catalysts. Fig. 2 shows the temperature profile in a cross section at the axial position $z = 2.54$ mm (z represents the axial distance from the bed inlet). In the modeling with the graphical interface, the scale on the graph is in millimeters, representing the actual dimensions of the reactor channels and the structured catalysts. It can be seen that the catalyst DF structures gave very narrow temperature distribution in the cross-section at a typical operating condition (850 °C, 20 atm, steam/C ratio = 2, 13.8 ms contact time, 72% methane conversion). The local cold spots typically inherent in conventional fixed bed reactors have been eliminated. Such improved heat transfer ensures the catalyst is being operated at an average high temperature that is close to the reactor wall temperature. On the contrary, catalyst C showed a large temperature gradient, in which numerous cold spots occur. The maximum temperature gradient was found to be 13 °C, which indicates that the catalyst located at the center part of the form in catalyst C is not optimally used. Consequently, the overall conversion is low.

Fig. 3 shows the local methane concentration profiles at a certain distance from the reactor inlet in the axial direction. The methane partial pressure was illustrated on the surface plots in concentration form with a unit of mol/mm^3. It can be seen that the conversion distribution is not uniform in both gas and solid phases. The local conversion is directly associated with, and in contrast to, the local temperature distribution shown in Fig. 2. The concentration gradient is predominantly caused by the increased Knudsen diffusion resistance in the catalyst layers with a pore radius of 50 Å. Additionally, the convection in the gas phase, which is equivalent to the effect of "bypass," also attributes to the synergistically mitigated rate. The integral value of the local concentration gives average conversion at the particular axial position. The overall conversion is subsequently the integrated value at the reactor exit. Fig. 4 shows the accumulated conversion profiles along the reactor length (axial z direction). Such numerical analysis quantitatively indicates that catalyst DF would yield much higher total conversion (70%) than

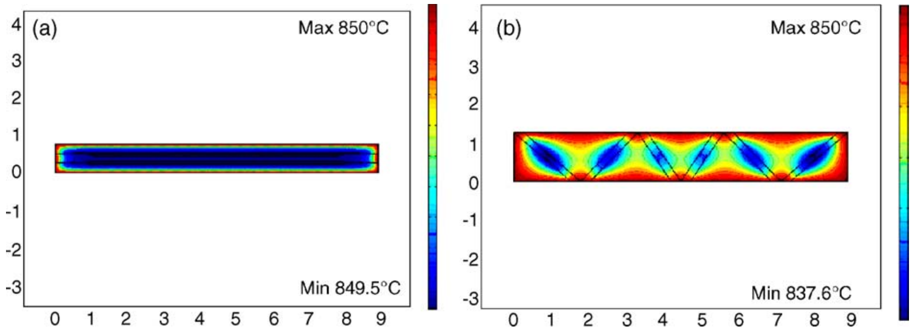

Fig. 2. Temperature distribution in a cross-section of methane steam reforming microchannel reactor ($z = 2.54$ mm, 13.8 ms contact time, 850 °C, 20 atm, steam/C = 2) for (a) catalyst DF and (b) catalyst C.

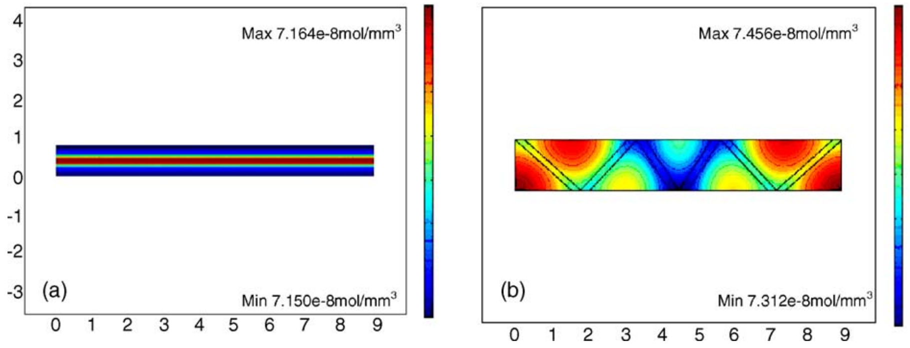

Fig. 3. Local methane concentration profile in a methane steam reforming microchannel reactor ($z = 2.54$ mm, 13.8 ms contact time, 850 °C, 20 atm, steam/C = 2) for (a) catalyst DF and (b) catalyst C.

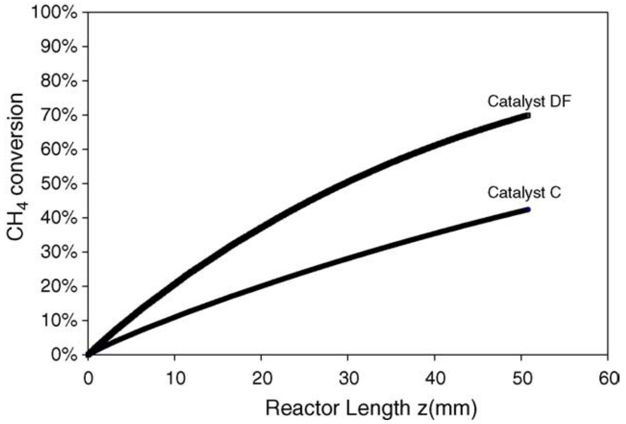

Fig. 4. Methane conversion along the reactor length (850 °C, 20 atm, steam/C = 2, 13.8 ms contact time).

catalyst C (42%). The results agree with the experimental data from a test at 13.8 ms contact time, particularly with catalyst DF. It is noticed that assumptions used in the model attribute to the deviation of model prediction from experimental results, particularly for catalyst type C that involves more complexity from its geometry and hydrodynamics.

This reactor model can be used to evaluate various catalyst structures in a microchannel reactor, as the geometry of the catalyst configuration can easily be altered with the convenient graphical interface. Sensitivity studies by varying the model parameters allow the catalyst properties such as pore size and coating thickness to be tailored to reduce the mass/heat transfer limitation.

5. Conclusions

A heterogeneous reactor model has been applied to evaluate microstructured catalysts for methane steam reforming. This approach demonstrates from a fundamental basis that structured catalysts and microchannel reactor integration provide advanced transport characteristics. Both simulation and experiments have validated the concept of the process intensification for such a diffusion controlled and highly endothermic steam reforming reaction. Two types of microstructured catalysts were evaluated, and their performance was differentiated by local conversion and temperature distributions. The heterogeneous model provides the three-dimensional view of microstructured catalyst beds, in which the roles of numerous variables and their interactions are presented. The model is of particular interest for designing new structured catalysts and choosing engineered substrates, particularly for optimizing the performances of microchannel reactors.

Acknowledgments

This work was performed in the Environmental Molecular Sciences Laboratory, a national scientific user facility sponsored by the US Department of Energy's Office of Biological and Environmental Research and located at Pacific Northwest National Laboratory in Richland, WA.

References

[1] F. Marschner, H.J. Renner, W. Boll, Electronic Encyclopedia, Release 2005, seventh ed. in: M. Bohnet, et al. (Eds.), Ullmann's Encyclopedia of Industrial Chemistry, vol. a12, John Wiley & Sons, 2005.
[2] J.R. Rostrup-Nielsen, I. Dybkjaer, G.R.G. Coulthard, Topical Conf. Proc. AIChE Spring National Meeting, Houston, TX, April, 2001, Paper No. 1.
[3] J.R. Rostrup-Nielsen, Steam Reforming Catalysts, Danish Technical Press, 1975,, p. 27.
[4] J.R. Rostrup-Nielsen, Catal. Rev. 46 (3–4) (2004) 247.
[5] W. Ehrfeld, V. Hessel, H. Lowe, Microreactor, Wiley-VCH Verlag GmbH, D-69469, Weinheim, 2000.
[6] K.F. Jensen, Chem. Eng. J. 56 (2001) 293.
[7] K. Schubert, J. Brandner, M. Fichtner, G. Linder, U. Schyhulla, A. Wenka, Microscale Thermophys. Eng. 5 (2001) 17.
[8] J.J. Lerou, K.M. Ng, Chem. Eng. Sci. 51 (10) (1996) 1595.
[9] J.D. Holladay, Y. Wang, E. Jones, Chem. Rev. 104 (10) (2004) 4767.
[10] Y. Wang, B.R. Johnson, C. Cao, Y. Chin, R.T. Rozmiarek, Y. Gao, A.L.Tonkovich, Engineered catalysts for microchannel reactor applications, in: Y. Wang, J. Holladay (Eds.), Microreactor Technology and Process Intensification, ACS Symposium Series, vol. 914, 2005.
[11] J.R. Rostrup-Nielsen, Catalysis: Science and Technology, vol. 5, Springer-Verlag, New York, 1984, p. 1.
[12] G.W. Bridger, Catalysis: Specialists Periodical Reports, vol. 3, The Chemical Society of London, 1980,, p. 39.
[13] J.R. Rostrup-Nielsen, L.J. Christiansen, J.H. BakHansen, Appl. Catal. 43 (1988) 287.
[14] H.M. Kvamsdal, H.F. Svendsen, T. Hertzberg, O. Olsvik, Chem. Eng. Sci. 54 (1999) 2697.

[15] R.M. Quinta Ferreira, M.M. Marques, M.F. Babo, A.E. Rodrigues, Chem. Eng. Sci. 47 (1992) 2909.

[16] S.S.E.H. Elnashaie, S.S. Elshishini, Modeling, Simulation and Optimization of Industrial Catalytic Fixed Bed Reactors, Gordon and Breach, Amsterdam, The Netherlands, 1993.

[17] J. Xu, G.F. Froment, AIChE J. 35 (1) (1989) 97.

[18] W.W. Akers, D.P. Camp, AIChE J. 1 (1955) 471.

[19] D.W. Allen, E.R. Gerhard, M.R. Likins Jr., Ind. Eng. Chem. Proc. Des. Dev. 14 (3) (1975) 256.

[20] L. Aparicio, J. Catal. 165 (1997) 262.

[21] Luna, A.M. Becerra, React. Kinet. Catal. Lett. 61 (2) (1997) 369.

[22] R. Craciun, B. Shereck, R.J. Gorte, Catal. Lett. 51 (3–4) (1998) 149.

[23] J. Xu, G.F. Froment, AIChE J. 35 (1) (1989) 88.

[24] A.E.C. Luna, A.M. Becerra, M.I. Dimitrijewits, React. Kinet. Catal. Lett. 67 (2) (1999) 247.

[25] J. Wei, I. Enrique, J. Phy. Chem. B 108 (13) (2004) 4094.

[26] Y. Wang, Y. Chin, R.T. Rozmiarek, B.R. Johnson, Y. Gao, J. Watson, A.L. Tonkovich, D.P. Vander Wiel, Catal. Today 98 (4) (2004) 575.

[27] K. Polychronopoulou, J.L.G. Fierro, A.M. Efstathiou, J. Catal. 228 (2) (2004) 417.

[28] R.C. Reid, J.M. Prausnitz, B.E. Poling, The Properties of Gases and Liquids, fourth ed., McGraw-Hill, New York, 1987.

[29] A.J.Fuller, T. Kim, H.P. Hodson, T.J. Lu, Cambridge Centre for Micromechanics Technical Report Archives, University of Cambridge.